Z. Phys. C – Particles and Fields 53, 41–49 (1992)

Zeitschrift für Physik C Particles and Fields

Search for excited charged leptons in Z^0 decays

DELPHI Collaboration

P. Abreu[16], W. Adam[42], F Adami[33], T. Adye[31], T. Akesson[19], G.D. Alekseev[12], P. Allen[41], S. Almehed[19], F. Alted[41], S.J. Alvsvaag[4], U. Amaldi[7], E. Anassontzis[3], P. Antilogus[20], W-D. Apel[13], B. Åsman[37], P. Astier[18], J-E. Augustin[15], A. Augustinus[7], P. Baillon[7], P. Bambade[15], F. Barao[16], G. Barbiellini[39], D.Y. Bardin[12], A. Baroncelli[34], O. Barring[19], W. Bartl[42], M.J. Bates[29], M. Baubillier[18], K-H. Becks[44], C.J. Beeston[29], M. Begalli[10], P. Beilliere[6], Yu. Belokopytov[36], P. Beltran[9], D. Benedic[8], J.M. Benlloch[41], M. Berggren[37], D. Bertrand[2], S. Biagi[17], F. Bianchi[38], J.H. Bibby[29], M.S. Bilenky[12], P. Billoir[18], J. Bjarne[19], D. Bloch[8], S. Blyth[29], P.N. Bogolubov[12], T. Bolognese[33], M. Bonapart[26], M. Bonesini[24], W. Bonivento[24], P.S.L. Booth[17], M. Boratav[18], P. Borgeaud[33], G. Borisov[36], H. Borner[29], C. Bosio[34], O. Botner[40], B. Bouquet[15], M. Bozzo[10], S. Braibant[7], P. Branchini[34], K.D. Brand[30], R.A. Brenner[11], C. Bricman[2], R.C.A. Brown[7], N. Brummer[26], J-M. Brunet[6], L. Bugge[28], T. Buran[28], H. Burmeister[7], J.A.M.A. Buytaert[2], M. Caccia[7], M. Calvi[24], A.J. Camacho Rozas[35], J-E. Campagne[7], A. Campion[17], T. Camporesi[7], V. Canale[32], F. Cao[2], L. Carroll[17], C. Caso[10], E. Castelli[39], M.V. Castillo Gimenez[41], A. Cattai[7], F.R. Cavallo[5], L. Cerrito[32], P. Charpentier[7], P. Checchia[30], G.A. Chelkov[12], L. Chevalier[33], P. Chliapnikov[36], V. Chorowicz[18], R. Cirio[38], M.P. Collins[29], J.L. Contreras[21], R. Contri[10], G. Cosme[15], F. Couchot[15], H.B. Crawley[1], D. Crennell[31], G. Crosetti[10], N. Crosland[29], M. Crozon[6], J. Cuevas Maestro[35], S. Czellar[11], S. Dagoret[15], E. Dahl-Jensen[25], B. Dalmagne[15], M. Dam[7], G. Damgaard[25], G. Darbo[10], E. Daubie[2], P.D. Dauncey[29], M. Davenport[7], P. David[18], A. De Angelis[39], M. De Beer[33], H. De Boeck[2], W. De Boer[13], C. De Clercq[2], M.D.M. De Fez Laso[41], N. De Groot[26], C. De La Vaissiere[18], B. De Lotto[35], A. De Min[24], C. Defoix[6], D. Delikaris[7], S. Delorme[7], P. Delpierre[6], N. Demaria[38], J. Derkaoui[38,22], L. Di Ciaccio[32], H. Dijkstra[7], F. Djama[8], J. Dolbeau[6], M. Donszelmann[26], K. Doroba[43], M. Dracos[7], J. Drees[44], M. Dris[27], Y. Dufour[6], W. Dulinski[8], R. Dzhelyadin[36], L-O. Eek[40], P.A.-M. Eerola[11], T. Ekelof[40], G. Ekspong[37], A. Elliot Peisert[30], J.P. Engel[8], V. Falaleev[36], D. Fassouliotis[27], M. Fernandez Alonso[35], A. Ferrer[41], T.A. Filippas[27], A. Firestone[1], H. Foeth[7], E. Fokitis[27], P. Folegati[39], F. Fontanelli[10], H. Forsbach[41], B. Franek[31], P. Frenkiel[6], D.C. Fries[13], A.G. Frodesen[4], R. Fruhwirth[42], F. Fulda-Quenzer[15], K. Furnival[17], H. Furstenau[13], J. Fuster[7], J.M. Gago[16], G. Galeazzi[30], D. Gamba[38], C. Garcia[41], J. Garcia[35], U. Gasparini[30], P. Gavillet[7], E.N. Gazis[27], J-P. Gerber[8], P. Giacomelli[5], K-W. Glitza[44], R. Gokieli[7], V.M. Golovatyuk[12], J.J. Gomez Y Cadenas[7], A. Goobar[37], G. Gopal[31], M. Gorski[43], V. Gracco[10], A. Grant[7], F. Grard[2], E. Graziani[34], M-H. Gros[15], G. Grosdidier[15], B. Grossetete[18], S. Gumenyuk[36], J. Guy[31], F. Hahn[7], M. Hahn[13], S. Haider[26], Z. Hajduk[26], A. Hakansson[19], A. Hallgren[40], K. Hamacher[44], G. Hamel De Monchenault[33], F.J. Harris[29], B.W. Heck[7], I. Herbst[44], J.J. Hernandez[41], P. Herquet[2], H. Herr[7], I. Hietanen[11], E. Higon[41], H.J. Hilke[7], S.D. Hodgson[29], T. Hofmokl[43], R. Holmes[1], S-O. Holmgren[37], D. Holthuizen[26], P.F. Honore[6], J.E. Hooper[25], M. Houlden[17], J. Hrubec[42], P.O. Hulth[37], K. Hultqvist[37], D. Husson[8], B.D. Hyams[7], P. Ioannou[3], D. Isenhower[7], P-S. Iversen[4], J.N. Jackson[17], P. Jalocha[14], G. Jarlskog[19], P. Jarry[33], B. Jean-Marie[15], E.K. Johansson[37], D. Johnson[17], M. Jonker[7], L. Jonsson[19], P. Juillot[8], G. Kalkanis[3], G. Kalmus[31], G. Kantardjian[7], F. Kapusta[18], S. Katsanevas[3], E.C. Katsoufis[27], R. Keranen[11], J. Kesteman[2], B.A. Khomenko[12], N.N. Khovanski[12], B. King[17], N.J. Kjaer[25], H. Klein[7], W. Klempt[7], A. Klovning[4], P. Kluit[26], J.H. Koehne[13], B. Koene[26], P. Kokkinias[9], M. Kopf[13], M. Koratzinos[7], K. Korcyl[14], A.V. Korytov[12], B. Korzen[7], V. Kostukhin[36], C. Kourkoumelis[3], T. Kreuzberger[42], J. Krolikowski[43], U. Kruener-Marquis[44], W. Krupinski[14], W. Kucewicz[24], K. Kurvinen[11], C. Lacasta[41], C. Lambropoulos[9], J.W. Lamsa[1], L. Lanceri[39], V. Lapin[36], J-P. Laugier[33], R. Lauhakangas[11], G. Leder[42], F. Ledroit[6], J. Lemonne[2], G. Lenzen[44], V. Lepeltier[15], A. Letessier-Selvon[18], D. Liko[42], E. Lieb[44], E. Lillethun[4], J. Lindgren[11], A. Lipniacka[43], I. Lippi[30], R. Llosa[21], B. Loerstad[19], M. Lokajicek[12], J.G. Loken[29], M.A. Lopez Aguera[35], A. Lopez-Fernandez[15], M. Los[26], D. Loukas[9], A. Lounis[8], J.J. Lozano[41], R. Lucock[31], P. Lutz[6], L. Lyons[29], G. Maehlum[7], J. Maillard[6], A. Maltezos[9], S. Maltezos[27], F. Mandl[42], J. Marco[35], M. Margoni[30], J-C. Marin[7], A. Markou[9], S. Marti[41], L. Mathis[6], F. Matorras[35], C. Matteuzzi[24], G. Matthiae[32], M. Mazzucato[30], M. Mc Cubbin[17], R. Mc Kay[1], R. Mc Nulty[17], E. Menichetti[38], C. Meroni[24], W.T. Meyer[1], M. Michelotto[30], W.A. Mitaroff[42], G.V. Mitselmakher[12], U. Mjoernmark[19], T. Moa[37], R. Moeller[25], K. Moenig[44], M.R. Monge[10], P. Morettini[10], H. Mueller[13], H. Muller[7], W.J. Murray[31], G. Myatt[29], F. Naraghi[18], U. Nau-Korzen[44], F.L. Navarria[5], P. Negri[24], B.S. Nielsen[25], B. Nijjhar[17], V. Nikolaenko[36], V. Obraztsov[36], A.G. Olshevski[12], R. Orava[11], A. Ostankov[36], A. Ouraou[33], R. Pain[18], H. Palka[26], T. Papadopoulou[27], L. Pape[7], A. Passeri[34], M. Pegoraro[30], V. Perevozchikov[36], M. Pernicka[42], A. Perrotta[5], F. Pierre[33], M. Pimenta[16], O. Pingot[2], A. Pinsent[29], M.E. Pol[16], G. Polok[14], P. Poropat[39], P. Privitera[13], A. Pullia[24], J. Pyythia[11], D. Radojicic[29], S. Ragazzi[24], W.H. Range[17], P.N. Ratoff[29], A.L. Read[28], N.G. Redaelli[24], M. Regler[42], D. Reid[17], P.B. Renton[29], L.K. Resvanis[3], F. Richard[15], M. Richardson[17], J. Ridky[12], G. Rinaudo[38], I. Roditi[7], A. Romero[38],

I. Roncagliolo[10], P. Ronchese[30], C. Ronnqvist[11], E.I. Rosenberg[1], U. Rossi[5], E. Rosso[7], P. Roudeau[15], T. Rovelli[5], W. Ruckstuhl[26], V. Ruhlmann[33], A. Ruiz[35], K. Rybicki[14], H. Saarikko[11], Y. Sacquin[33], J. Salt[41], E. Sanchez[41], J. Sanchez[21], M. Sannino[10], M. Schaeffer[8], H. Schneider[13], F. Scuri[39], A.M. Segar[29], R. Sekulin[31], M. Sessa[39], G. Sette[10], R. Seufert[13], R.C. Shellard[16], P. Siegrist[33], S. Simonetti[10], F. Simonetto[30], A.N. Sissakian[12], T.B. Skaali[28], G. Skjevling[28], G. Smadja[33,20], G.R. Smith[31], N. Smirnov[36], R. Sosnowski[43], T.S. Spassoff[12], E. Spiriti[34], S. Squarcia[10], H. Staeck[44], C. Stanescu[34], G. Stavropoulos[9], F. Stichelbaut[2], A. Stocchi[15], J. Strauss[42], R. Strub[8], C.J. Stubenrauch[7], M. Szczekowski[43], M. Szeptycka[43], P. Szymanski[43], T. Tabarelli[24], S. Tavernier[2], G.E. Theodosiou[9], A. Tilquin[23], J. Timmermans[26], V.G. Timofeev[12], L.G. Tkatchev[12], T. Todorov[12], D.Z. Toet[26], L. Tortora[34], M.T. Trainor[29], D. Treille[7], U. Trevisan[10], W. Trischuk[7], G. Tristram[6], C. Troncon[24], A. Tsirou[7], E.N. Tsyganov[12], M. Turala[14], R. Turchetta[8], M-L. Turluer[33], T. Tuuva[11], I.A. Tyapkin[12], M. Tyndel[31], S. Tzamarias[7], B. Ueberschaer[44], S. Ueberschaer[44], O. Ullaland[7], V.A. Uvarov[36], G. Valenti[5], E. Vallazza[38], J.A. Valls Ferrer[41], G.W. Van Apeldoorn[26], P. Van Dam[26], W.K. Van Doninck[2], N. Van Eijndhoven[7], C. Vander Velde[2], J. Varela[16], P. Vaz[16], G. Vegni[24], J. Velasco[41], L. Ventura[30], W. Venus[31], F. Verbeure[2], L.S. Vertogradov[12], L. Vibert[18], D. Vilanova[33], E.V. Vlasov[36], A.S. Vodopyanov[12], M. Vollmer[44], S. Volponi[5], G. Voulgaris[3], M. Voutilainen[11], V. Vrba[34], H. Wahlen[44], C. Walck[37], F. Waldner[39], M. Wayne[1], P. Weilhammer[7], J. Werner[44], A.M. Wetherell[7], J.H. Wickens[2], J. Wikne[28], G.R. Wilkinson[29], W.S.C. Williams[29], M. Winter[8], D. Wormald[28], G. Wormser[15], K. Woschnagg[40], N. Yamdagni[37], P. Yepes[7], A. Zaitsev[36], A. Zalewska[14], P. Zalewski[43], E. Zevgolatakos[9], G. Zhang[44], N.I. Zimin[12], M. Zito[33], R. Zitoun[18], R. Zukanovich Funchal[6], G. Zumerle[30], J. Zuniga[41]

[1] Ames Laboratory and Department of Physics, Iowa State University, Ames IA 50011, USA
[2] Physics Department, Univ. Instelling Antwerpen, Universiteitsplein 1, B-2610 Wilrijk, Belgium
and IIHE, ULB-VUB, Pleinlaan 2, B-1050 Brussels, Belgium
and Service de Phys. des Part. Elém., Faculté des Sciences, Université de l'Etat Mons, Av. Maistriau 19, B-7000 Mons, Belgium
[3] Physics Laboratory, University of Athens, Solonos Str. 104, GR-10680 Athens, Greece
[4] Department of Physics, University of Bergen, Allégaten 55, N-5007 Bergen, Norway
[5] Dipartimento di Fisica, Università di Bologna and INFN, Via Irnerio 46, I-40126 Bologna, Italy
[6] Collège de France, Lab. de Physique Corpusculaire, 11 pl. M. Berthelot, F-75231 Paris Cedex 05, France
[7] CERN, CH-1211 Geneva 23, Switzerland
[8] Division des Hautes Energies, CRN-Groupe DELPHI and LEPSI, B.P. 20 CRO, F-67037 Strasbourg Cedex, France
[9] Institute of Nuclear Physics, N.C.S.R. Demokritos, P.O. Box 60228, GR-15310 Athens, Greece
[10] Dipartimento di Fisica, Università di Genova and INFN, Via Dodecaneso 33, I-16146 Genova, Italy
[11] Research Institute for High Energy Physics, University of Helsinki, Siltavuorenpenger 20 C, SF-00170 Helsinki 17, Finland
[12] Joint Institute for Nuclear Research, Dubna, Head Post Office, P.O. Box 79, 101000 Moscow, USSR
[13] Institut für Experimentelle Kernphysik, Universität Karlsruhe, Postfach 6980, W-7500 Karlsruhe 1, Federal Republic of Germany
[14] High Energy Physics Laboratory, Institute of Nuclear Physics, Ul. Kawiory 26a, PL-30055 Krakow 30, Poland
[15] Université de Paris-Sud, Lab. de l'Accélérateur Linéaire, Bat 200, F-91405 Orsay, France
[16] LIP, Av. Elias Garcia 14-1e, P-1000 Lisbon Codex, Portugal
[17] Department of Physics, University of Liverpool, P.O. Box 147, GB-Liverpool L69 3BX, UK
[18] LPNHE, Universités Paris VI et VII, Tour 33 (RdC), 4 place Jussieu, F-75230 Paris Cedex 05, France
[19] Department of Physics, University of Lund, Sölvegatan 14, S-22363 Lund, Sweden
[20] Université Claude Bernard de Lyon, 43 Bd du 11 Novembre 1918, F-69622 Villeurbanne Cedex, France
[21] Departamento de Fisica Atomica Moleculary y Nuclear, Universidad Complutense, Avda, Complutense s/n, E-28040 Madrid, Spain
[22] Département de Physique, Faculté des Sciences d'Oujda, Maroc
[23] Faculté des Sciences de Luminy, Univ. d'Aix – Marseille II Case 907–70, route Léon Lachamp, F-13288 Marseille Cedex 09, France
[24] Dipartimento di Fisica, Università di Milano and INFN, Via Celoria 16, I-20133 Milan, Italy
[25] Niels Bohr Institute, Blegdamsvej 17, DK-2100 Copenhagen 0, Denmark
[26] NIKHEF-H, Postbus 41882, NL-1009 DB Amsterdam, The Netherlands
[27] National Technical University, Physics Department, Zografou Campus, GR-15773 Athens, Greece
[28] Physics Department, University of Oslo, Blindern, N-1000 Oslo 3, Norway
[29] Nuclear Physics Laboratory, University of Oxford, Keble Road, GB – Oxford OX1 3RH, UK
[30] Dipartimento di Fisica, Università di Padova and INFN, Via Marzolo 8, I-35131 Padua, Italy
[31] Rutherford Appleton Laboratory, Chilton, GB – Didcot OX11 OQX, UK
[32] Dipartimento di Fisica, Università di Roma II and INFN, Tor Vergata, I-00173 Rome, Italy
[33] CEN-Saclay, DPhPE, F-91191 Gif-sur-Yvette Cedex, France
[34] Istituto Superiore di Sanità, Ist. Naz. di Fisica Nucl. (INFN), Viale Regina Elena 299, I-00161 Rome, Italy
[35] Facultad de Ciencias, Universidad de Santander, av. de los Castros, E-39005 Santander, Spain
[36] Inst. for High Energy Physics, Serpukow P.O. Box 35, Protvino, (Moscow Region), USSR
[37] Institute of Physics, University of Stockholm, Vanadisvägen 9, S-11346 Stockholm, Sweden
[38] Dipartimento di Fisica Sperimentale, Università di Torino and INFN, Via P. Giuria 1, I-10125 Turin, Italy
[39] Dipartimento di Fisica, Università di Trieste and INFN, Via A. Valerio 2, I-34127 Trieste, Italy
and Istituto di Fisica, Università di Udine, I-33100 Udine, Italy
[40] Department of Radiation Sciences, University of Uppsala, P.O. Box 535, S-75121 Uppsala, Sweden
[41] Inst. de Fisica Corpuscular IFIC, Centro Mixto Univ. de Valencia-CSIC, Avda. Dr. Moliner 50, E-46100 Burjassot (Valencia), Spain
[42] Institut für Hochenergiephysik, Oesterreich Akad. d. Wissensch., Nikolsdorfergasse 18, A-1050 Vienna, Austria
[43] Inst. Nuclear Studies and University of Warsaw, Ul. Hoza 69, PL-00681 Warsaw, Poland
[44] Fachbereich Physik, University of Wuppertal, Postfach 100127, W-5600 Wuppertal 1, Federal Republic of Germany

Received 28 August 1991

Abstract. Using a data sample of 115000 hadronic Z^0 decays, a search was performed for the production of excited charged leptons decaying into an ordinary lepton and one photon. Pair production of excited leptons of mass below 45 GeV/c^2 is excluded. From an analysis of the lepton-photon mass spectra this experiment is also able to exclude single production of these particles for masses that reach up to 85 GeV/c^2, if the compositeness scale is below 1 TeV.

1 Introduction

This paper presents a systematic search for unstable heavy excited charged leptons assumed to decay into a normal lepton and a photon. The decays of Z^0's produced at LEP are investigated to look for acollinear two-prong events with at least one photon visible in the electromagnetic calorimeters.

Compositeness [1] provides a general framework which describes the coupling of the photon and Z^0 to excited leptons. One may assume that they have the same weak isospin properties as ground state leptons and, consequently, are pair-produced with standard cross sections and angular distributions. Single production of an excited lepton could also be possible, however, with unknown $l^* lZ$ and $l^* l\gamma$ couplings. As pointed out in reference [2], the single production of excited electrons is greatly enhanced by the contribution of the diagram corresponding to photon exchange in the t-channel. In this process the spectator electron tends to be emitted at very small angles with respect to the beam direction and escapes the detector. In order to be sensitive also to this process, the search has been extended to $e\gamma$ final states.

The main background affecting the present search comes from leptonic decays of the Z^0 with radiation of one or more energetic photons. This background can be substantially reduced by demanding that the photons be isolated from the leptons but, ultimately, the l^* candidates have to be distinguished by looking for a narrow peak in $l^{\pm}\gamma$ mass combinations. For the allowed range of l^* couplings, the width of these particles is expected to be much smaller than the mass resolution of the detector. Standard mass reconstruction of l^* which uses the measured momenta and angles of leptons and photons is inadequate for the channel $\tau^+\tau^-\gamma$. However, as the τ's are energetic, their directions are approximately given by their daughter particles so their momenta can be calculated using energy-momentum conservation. The method is very precise and was also used in this analysis for the $ee\gamma$, $\mu\mu\gamma$ and $e\gamma$ channels.

2 Apparatus

A detailed description of the DELPHI detector, of the triggering conditions and of the analysis chain can be found in [3]. Here, only the specific properties relevant to the following analysis are summarized.

The charged particle tracks are measured in the 1.2 T magnetic field by a set of three cylindrical tracking detectors: the inner detector (ID) covers radii 12 to 22 cm, the time projection chamber (TPC) from 28 to 122 cm, and the outer detector (OD) between 192 and 208 cm. The end caps are covered by the forward chambers A and B, at polar angles θ between 10° and 36° on each side. A layer of time-of-flight (TOF) counters is installed for triggering purposes beyond the magnet coil.

The electromagnetic energy is measured by the high density projection chamber (HPC) in the barrel region, and by the forward electromagnetic calorimeter (FEMC) in the end caps. The HPC is a high granularity gaseous calorimeter covering polar angles 40° to 140°. For fast triggering a layer of scintillation counters is installed after the first 5 radiation lengths of lead. The FEMC consists of 2·4500 lead glass blocks (granularity 1·1 degrees), covering polar angles from 10° to 36° on each side. The small angle tagger calorimeter (SAT) is an electromagnetic calorimeter covering polar angles from 43 to 125 mrad in the forward and backward directions. It is composed of alternate layers of lead sheets and scintillating fibres parallel to the beams and it provides the measurement of luminosity.

Muons and hadrons are identified using the forward and barrel hadron calorimeters (HCAL) which cover $10° \leqq \theta \leqq 170°$, followed by muon chambers which cover $10° \leqq \theta \leqq 45°$, $51° \leqq \theta \leqq 129°$ and $135° \leqq \theta \leqq 170°$. The total amount of iron traversed varies from 5 to 7 interactions lengths.

The trigger is based on signals from the inner and outer detectors, the HPC and TOF scintillation counters, and the forward detectors. These signals are combined in several sets of coincidence, back-to-back and majority logics. The logical OR of the various subtriggers provides a high redundancy for events of the type studied in this analysis, in which high-momentum charged tracks and high-energy photons are simultaneously present.

3 Event analysis

The data presented here have been collected during the energy scans performed at LEP during 1990. Only those runs where all the essential subdetectors were fully operational were used; they correspond to a total of about 115000 registered Z^0 decays.

Charged tracks are retained in the analysis if they have a momentum greater than 100 MeV/c and are emitted at more than 25° with respect to the beam axis, where tracks are well reconstructed by the TPC. They must also come from the interaction point to within 10 cm in the longitudinal coordinate and 2 cm in the radial direction.

To define a photon, a cluster is required in the HPC or the FEMC with a total energy deposit above 2 GeV and at more than 25° with respect to the beam axis. It is also demanded that this photon is isolated, being emitted more than 15° from any charged particle. This cut removes many of the standard lepton pairs with final

state radiation and has little impact on the search for heavy excited lepton.

The identification of electrons is based on the comparison between the track momentum and the energy deposited in the electromagnetic calorimeters E_{em}. In order to distinguish primary electrons from those coming from τ decay, the momentum calculated by imposing energy-momentum conservation in the events p_{calc} was used; due to the missing energy carried away by the neutrinos, a cut requiring the value of E_{em}/p_{calc} to be close to one will reject the majority of secondary electrons.

Muon tagging is obtained by combining the information from the calorimeters and the muon chamber system. In order to be identified as a muon, a track must leave an energy deposit in both the electromagnetic and the hadron calorimeter compatible with that expected for a minimum ionizing particle, and/or be associated to at least two hits in the muon chambers. The overall identification efficiency is 90% per track.

The Z^0 decays to the various composite channels studied in this paper were generated using the detailed simulation program of DELPHI [4]. For background simulation, which requires much larger samples, a simplified program [5] was used, which was tuned to reproduce the experimental data.

Trigger efficiencies were measured for each of the individual subtriggers by analyzing the trigger pattern in leptonic Z^0 decays; these efficiencies were then used in the Monte Carlo simulation for all the relevant channels. The lowest trigger efficiency, $85 \pm 5\%$, corresponds to the $\mu\mu\gamma$ final state, for which the redundancy between the subtriggers based on charged tracks and those based on electromagnetic energy is smallest.

3.1 Pair production

Pair production of excited charged leptons having the same weak isospin as the standard leptons can be excluded for a large range of masses directly from the measurement of the Z^0 width. In [6] an upper limit of 28 MeV (at 95% c.l.) is given on any non-standard contribution to Γ_Z; this implies a lower limit of 33 GeV/c^2 on the mass of the l^*, completely independent of its decay properties.

For higher values of the l^* mass, a direct search was made for the process $Z^0 \to l^{*+} l^{*-}$ with $l^* \to l\gamma$. The selection asked for events having only two charged particles, each with momentum above 2 GeV/c, and two photons. The two charged particles should have an acollinearity angle between 10° and 170°. Due to the photon isolation cut, this direct analysis is sensitive only to excited leptons heavier than ~ 6 GeV/c^2.

Two events have been found. In one of them the less energetic photon does not point to the interaction vertex, and the remaining three particles are coplanar. It was therefore identified as a $\mu\mu\gamma$ event with an additional spurious hit in the HPC. The second event was confirmed as a four-particle event (Fig. 1). It was classified as an $ee\gamma\gamma$ event, since both charged particles are identified as electrons and the total measured energy is consistent

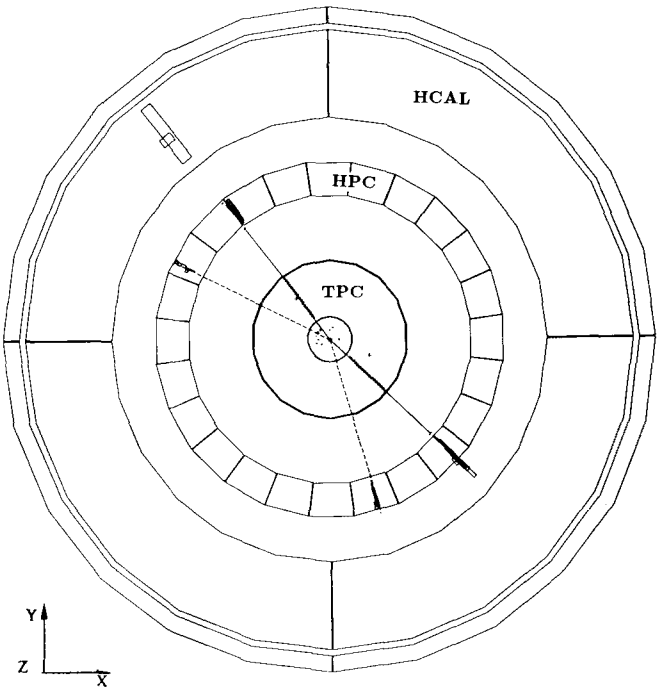

Fig. 1. Display of the $ee\gamma\gamma$ event in the plane perpendicular to the beams. The two electrons (continuous lines) and the two photons (dashed lines) produce showers in the HPC; part of the shower of one of the electrons leaks into the HCAL. (Run: 14854, event 1245)

Table 1. Invariant masses (in GeV/c^2) of the $e\gamma$ pairs for the $ee\gamma\gamma$ event

1st Combination		2nd Combination	
35.4 ± 1.4	27.7 ± 1.2	10.4 ± 0.5	8.8 ± 0.4

with the LEP energy. Table 1 shows the masses of the different $e\gamma$ combinations. Within the errors, the event is compatible with an $e^{*+} e^{*-}$ final state in the second combination, corresponding to an average mass of about 9.6 GeV/c^2, well within the region excluded by Γ_Z. The first combination appears to be excluded. However, the errors on the momentum of the electrons could be underestimated, since the bremsstrahlung inside the detector can induce an additional systematic contribution that is difficult to evaluate, so that a common mass of about 32 GeV/c^2 cannot be completely ruled out. The particle energies can be recalculated with greater precision from the measured angles between the four particles, using a 0-constraint fit. Since undetected radiation along the beam axis would induce an error in the result of the fit, the calculation was repeated with varying amounts of missing energy and momentum along this axis. It was found that no solution exists where both $e\gamma$ masses are above 36 GeV/c^2.

The expected number of selected events from $e^{*+} e^{*-}$ production at masses below 36 GeV/c^2 is over 500;

therefore, one can conclude that there is no evidence for this decay.

The efficiencies for the detection of e^* and μ^* pairs increase from $45 \pm 5\%$ at $m_{l^*} = 20$ GeV/c^2 to $50 \pm 5\%$ at the kinematical limit; for τ^* it is about $17 \pm 2\%$ over the whole mass range above 20 GeV/c^2.

To estimate the standard background, the program KORALZ [7] was used. It predicts 0.8 ± 0.1 $\mu\mu\gamma\gamma$ events within the selection cuts. However, this program does not include all the amplitudes for the radiation of two hard photons (the radiation of two photons in the final state is missing), so the quoted number is probably a lower limit on the expected background. No generator is available for $ee\gamma\gamma$, but one expects roughly the same number of events as for $\mu\mu\gamma\gamma$.

3.2 *Single production in annihilation*

The kinematics in this process allow the production of an l^* heavier than 45 GeV/c^2; for this higher masses, the photon isolation criterion has been strengthened. Two charged particles are required, each with momentum above 2 GeV/c, and one photon at more than 30° with respect to either of them. The two charged particles should have an acollinearity angle between 10° and 170°. To avoid large errors on the calculation of the mass due to initial state radiation, as explained below, the runs where the LEP energy was on the high tail of the Z^0 resonance were rejected; it was demanded that $2E_b \leqq M_Z + \Gamma_Z/2$, where E_b is the beam energy. After this selection, 151 events remain.

The momenta of the three final state particles are computed from the measured angles between the three particles, α_{12}, α_{13} and α_{23}, using energy-momentum conservation. Since in a genuine 3-body event the three particles must lie in a plane, the sum of these angles is required to be above 358°; this cut removes the background from two-photon interactions and very forward hadronic events. Monte Carlo simulation shows it affects only the $\tau^*\tau$ channel, where 3% of the events are lost. There are 118 events which pass this last cut.

To compute the momenta, the following formula was used:

$$\frac{p_1}{\sin\alpha_{23}} = \frac{p_2}{\sin\alpha_{13}} = \frac{p_3}{\sin\alpha_{12}} = \frac{2E_b}{\sin\alpha_{12} + \sin\alpha_{13} + \sin\alpha_{23}}.$$

Figure 2 shows the distribution of $l\gamma$ masses for the candidate events; there is a good agreement both in shape and normalization with the curve predicted by a Monte Carlo generation of 400000 standard leptonic decays of the Z^0 [8].

The excess around 80 GeV/c^2 is of low statistical significance and it is not dominated by any of the three lepton channels.

3.2.1 Channel identification. The final lepton channel is identified by relying on the particle identification and on the comparison between the measured momenta and those calculated with the above formula. Events are clas-

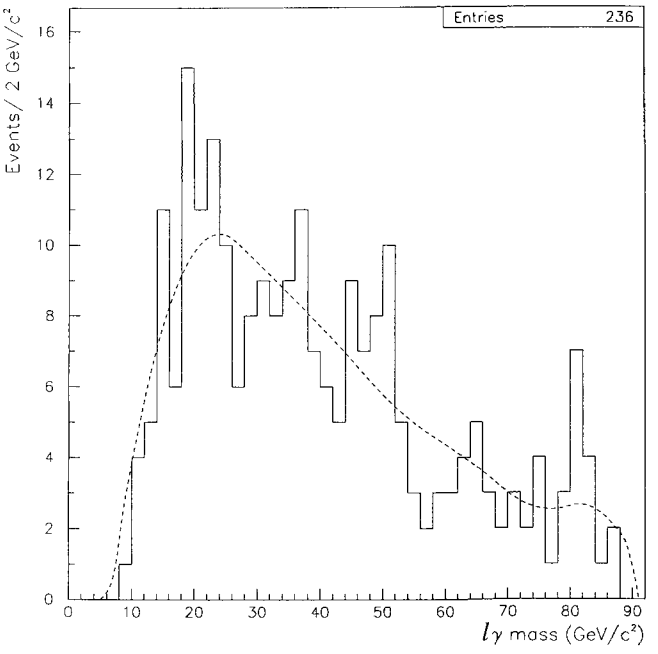

Fig. 2. Spectrum of $l\gamma$ masses for all $ll\gamma$ events (two entries per event). The line shows the shape predicted by a Monte Carlo simulation of standard decays of the Z^0 into two leptons plus a photon

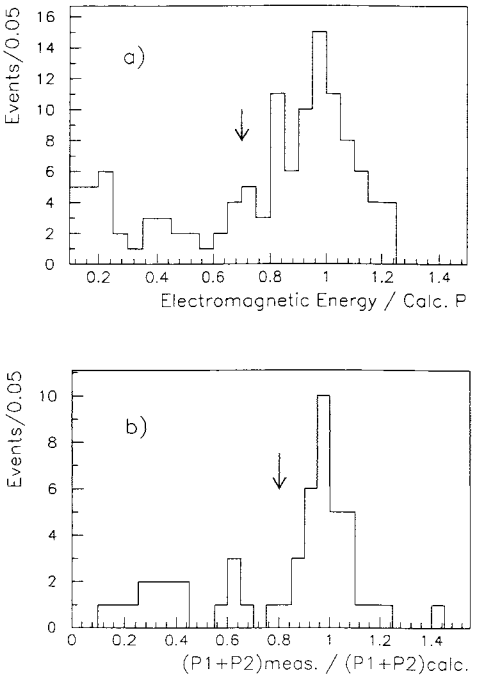

Fig. 3a, b. Distributions of the variables used to identify the lepton channel in $ll\gamma$ events. In both plots the arrows show the cuts used to identify the events, as explained in the text. **a** Ratio of the electromagnetic energy associated to each track to the momentum calculated for the track from the measured angles. **b** Ratio of the sum of measured momenta to the sum of calculated momenta for the two charged particles in events containing at least one muon candidate

Table 2. Number of $ll\gamma$ events found for each channel, and number of events expected from standard processes

Channel	Observed	Expected
$ee\gamma$	54	56 ± 4
$\mu\mu\gamma$	34	37 ± 3
$\tau\tau\gamma$	24	21.4 ± 1.7

sified as $ee\gamma$ if there is at least one charged particle identified as a primary electron, that is, for which E_{em}/p_{calc} falls in the peak above 0.7 (Fig. 3a). For $\mu\mu\gamma$ it is required that at least one of the charged particles be identified as a muon, and that the ratio of the sum of the two measured momenta to the sum of the calculated momenta be above 0.8 (Fig. 3b). The second requirement removes the background from $\tau\tau\gamma$ events. Finally, events are kept as $\tau\tau\gamma$ candidates if they do not show ee or $\mu\mu$ signatures and have at least one particle whose measured momentum is unambiguously below the computed value ($p_{meas}/p_{calc}<0.5$). Table 2 gives the number of events selected for each channel together with Monte Carlo expectations for the background from standard Z^0 decays.

3.2.2 Mass resolution. The angular resolution of the detector is the main factor that determines the mass resolution for e^* and μ^*, since the momenta are calculated from the measured angles. These resolutions have been measured for electrons, muons and photons by analyzing the acollinearity and acoplanarity distributions of e^+e^- and $\mu^+\mu^-$ events. The widths of these distributions are influenced by soft-photon radiation, but since this effect is also present in the $ll\gamma$ events and affects the mass resolution, no correction was made for it. Initial state radiation is limited by the resonant shape of the cross section, and it was further reduced by rejecting data taken above the Z^0 peak.

These experimentally measured resolutions were used in the Monte Carlo simulations of l^*l production, in which radiative effects were also included. The resolution is found to be ±250 MeV/c^2 for the $ee\gamma$ and $\mu\mu\gamma$ channels and ±2.0 GeV/c^2 for $\tau\tau\gamma$; the latter is dominated by the angle between the τ's and their daughter particles. These values are practically independent of the l^* mass.

An independent verification of the consistency between data and Monte Carlo can be obtained by studying the distributions of the product $(\hat{p}_1\times\hat{p}_2)\cdot\hat{p}_3$ of the unit vectors defined by the observed particles. This variable, which measures the coplanarity of the three particles, is sensitive to the same effects that define the mass resolution. As shown in Fig. 4, there is good agreement between data and the results of Monte Carlo simulation of standard Z^0 decays.

3.2.3 Results. Figures 5a, 6 and 7 show the observed mass distributions for the three channels; the binning has been chosen so that 80% of the signal from l^* decay would be concentrated in two bins. No apparent structure is seen. The acceptances of the present selection for the various channels are given in Table 3.

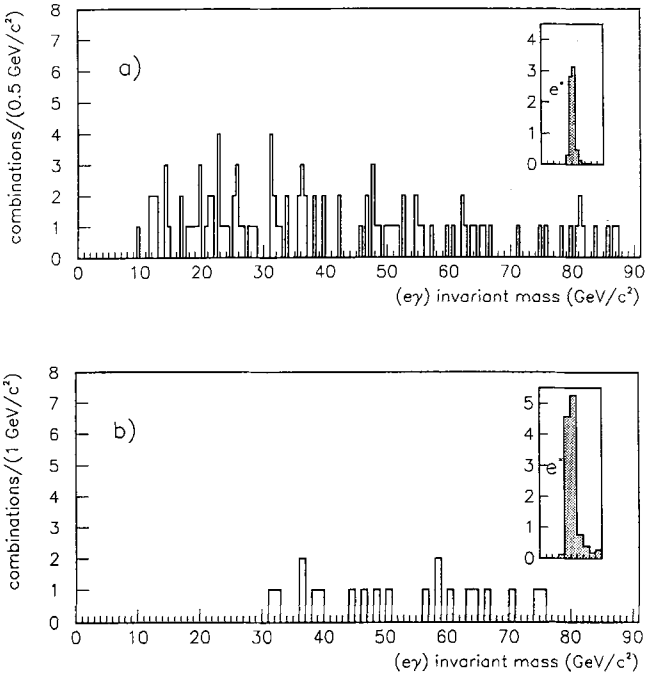

Fig. 5. Spectra of $e\gamma$ masses for the observed events. **a** $ee\gamma$ events (two entries per event). **b** $e(e)\gamma$ events. The windows in each plot show the expected signal for the production of an 80 GeV/c^2 e^* with $f/\Lambda=2$ TeV^{-1}

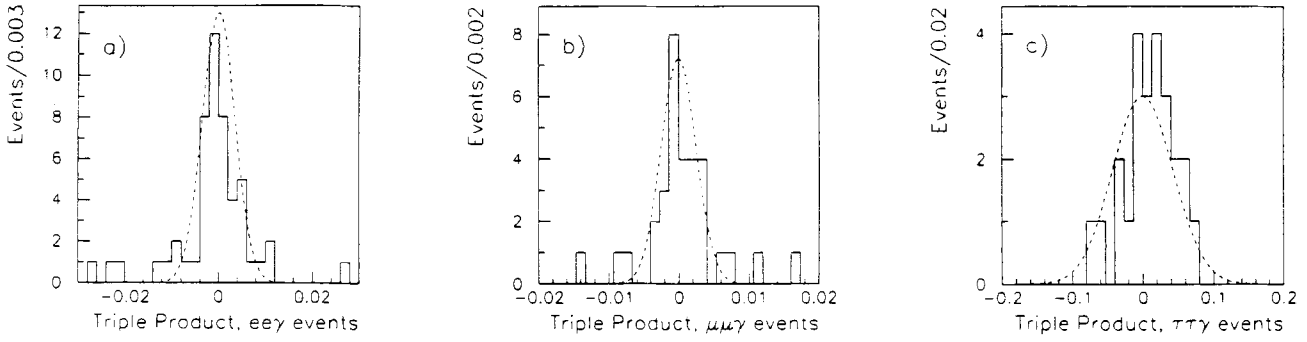

Fig. 4a–c. Distributions of the normalized triple product $(\hat{p}_1\times\hat{p}_2)\cdot\hat{p}_3$ for $ll\gamma$ events. The curves show the shape expected from a Monte Carlo generation for each channel. **a** $ee\gamma$, **b** $\mu\mu\gamma$, **c** $\tau\tau\gamma$

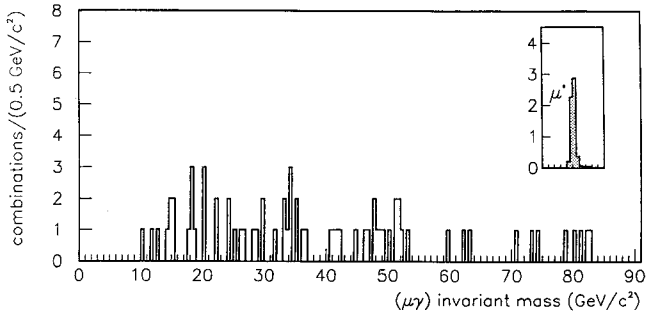

Fig. 6. Spectrum of $\mu\gamma$ masses for the observed $\mu\mu\gamma$ events (two entries per event). The window shows the expected signal for $m_{\mu^*} = 80$ GeV/c^2, $f/\Lambda = 2$ TeV^{-1}

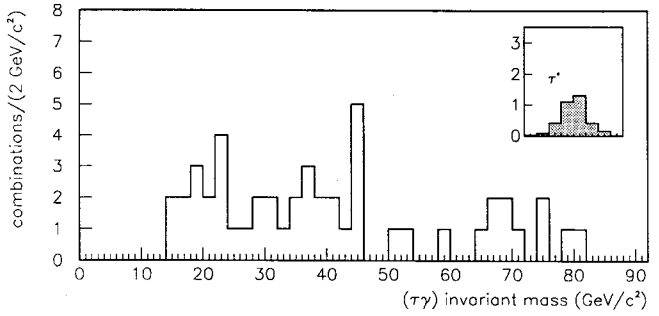

Fig. 7. Spectrum of $\tau\gamma$ masses for the observed $\tau\tau\gamma$ events (two entries per event). The window shows the expected signal for $m_{\tau^*} = 80$ GeV/c^2, $f/\Lambda = 2$ TeV^{-1}

Table 3. Detection efficiencies (in percent) for singly-produced excited leptons. Relative uncertainties are below 10%

	l^* mass (GeV/c^2)				
Channel	50	60	70	80	85
$ee\gamma$	48	47	49	49	50
$\mu\mu\gamma$	42	42	43	43	43
$\tau\tau\gamma$	28	28	28	25	16
$e(e)\gamma$	18	22	26	34	30

3.3 Single e production via t-channel exchange*

Excited electrons can be produced through photon exchange in the t-channel. In most cases, the spectator electron stays very near to the beam direction and remains invisible while the photon and electron from the decay of the e^* are back-to-back in the plane perpendicular to the beam. To select this type of event the following requirements are imposed: the event must have a single photon with energy above 8 GeV and a single charged particle with momentum above 5 GeV/c and an electromagnetic energy deposition above 2 GeV. The acollinearity angle between the two particles must be above 5°, to eliminate the background from $ee \to \gamma\gamma$ events where one of the photons converts before the TPC. Finally, to avoid contamination coming from e^+e^- events where one of the charged tracks is lost, only the photons in the barrel region ($40° < \theta < 140°$) are selected, and ϕ is restricted to be at more than 4° from the boundaries of the sectors of the TPC.

After these selections 24 candidates remain. The background from standard processes comes mainly from Compton scattering. It was computed using a Monte Carlo program where the photon flux is given by a Weizsäcker-Williams approximation (see for instance [9]), and which includes multiple initial-state radiation: 22 events are predicted, in good agreement with the data.

The computation of the mass from the angles is still possible assuming that the spectator electron is approximately aligned with the beam. The method is however affected by initial state radiation; to eliminate the events with energetic photons along the beam direction, a loose cut is imposed on the match between the missing energy and the missing longitudinal momentum. Demanding $|p^z_{\rm mis}|/E_{\rm mis} > 0.5$ rejects 4 events in agreement with Monte Carlo expectation. The resulting mass spectrum is shown in Fig. 5b; again, no peak is seen.

The acceptance of the present selection criteria for different e^* masses is given in the last line of Table 3. The mass resolution is 450 MeV/c^2, although there is a non-Gaussian tail due to radiation effects, as shown in the inset of Fig. 5b.

4 Limits on Compositeness

All the limits discussed in this section are based on the assumption that the decay branching ratio of an excited lepton into a standard lepton plus a photon is 100%.

Pair production allows one to derive direct limits on the masses if standard couplings of the l^* to the Z^0 are assumed.

As explained in Sect. 3.1, the only candidate event is in a mass region where the number of expected events is very high, so the limits obtained are not affected by it. The calculation of the expected number of events took into account the luminosities collected at each energy point for the total event sample considered in the analysis. The limits obtained are (at 95% confidence level):

$m_{e^*} > 45.6$ GeV/c^2
$m_{\mu^*} > 45.6$ GeV/c^2
$m_{\tau^*} > 45.3$ GeV/c^2.

These results do not depend on the compositeness scale, except that the $l^* l\gamma$ coupling is supposed to be strong enough to allow the l^* to decay inside the detector. However, a stable l^* can be excluded up to masses of 40 GeV/c^2 on the basis of a previous analysis [10].

Single production of an excited lepton is given in terms of unknown $l^* lZ$ and $l^* l\gamma$ couplings. The effective Lagrangian is of the form:

$$\mathcal{L} = \sum_{V=\gamma,Z^0} \frac{e}{2\Lambda} \bar{\Psi}_l \sigma^{\mu\nu}(c_V - d_V \gamma^5) \Psi_{l^*} F^V_{\mu\nu} + \text{h.c.}$$

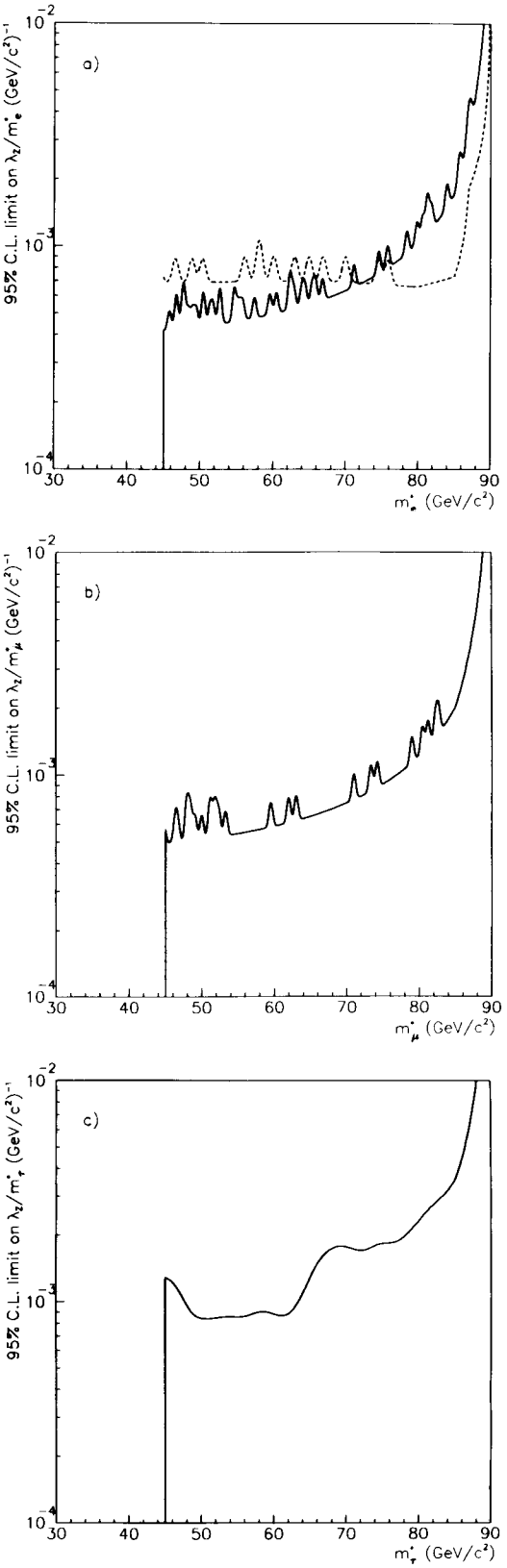

Fig. 8a–c. 95% confidence level limits on the minimum value of the effective scale for the l^*lZ and $l^*l\gamma$ couplings, expressed as a function of the l^* mass. **a** e^* couplings. The continuous and dashed lines correspond to the limits derived from the searches for production through Z^0 decay and through photon exchange in the t-channel, respectively. **b** μ^* couplings. **c** τ^* couplings. The regions above and to the left of the lines are excluded

where Λ is an arbitrary energy scale. CP-invariance imposes the condition that c_V and d_V be real, while $g-2$ measurements imply chirality conservation and hence $c_V = \pm d_V$ [11]. Explicitly, one finds the following expression for the production cross-section in Z^0 decay:

$$\sigma(\bar{l}^* l + \bar{l} l^*) = 16 \frac{s}{\Lambda^2}(c_Z^2 + d_Z^2)\cdot \sin^2\theta_W \cos^2\theta_W (1-x^2)^2 \cdot(1+2x^2)\,\sigma_{\nu\bar{\nu}}$$

where s is the square of the cm energy, θ_W the weak mixing angle, $x = m_{l^*}/m_{Z^0}$, and $\sigma_{\nu\bar{\nu}}$ the neutrino-antineutrino cross-section. The decay of l^* into $l\gamma$ has a $1+\cos\theta$ dependence due to chirality conservation.

The model of [2] allows c_γ, d_γ, c_Z and d_Z to be expressed in terms of two parameters, f and f', that specify the $SU(2)$ and $U(1)$ couplings respectively. With the assumption $f = f'$, the cross-section depends on a single variable, f/Λ. To allow easier comparison with limits obtained from other analyses, the limits from this experiment are presented in terms of the parameter λ/m_{l^*}, defined as:

$$\frac{\lambda}{m_{l^*}} = \frac{f}{\sqrt{2}\Lambda}$$

which was used in previous e^+e^- experiments testing the coupling of the l^* to the photon. The contours given in Fig. 8 show the limits (at 95% confidence level) on λ/m_{l^*} as a function of m_{l^*}. They take into account the mass resolution and the estimated background contributions from standard processes. For a value of the effective coupling λ/m_{l^*} equal to 1 TeV^{-1}, this analysis excludes e^* with masses below 85 GeV/c^2, μ^* below 77 GeV/c^2 and τ^* below 63 GeV/c^2. Similar limits have been obtained by the other LEP experiments [12]. A recent analysis of the e^+e^- annihilation into two photons [13] also excludes e^* in a mass range that extends above m_Z, although only for values of the effective coupling above 100 GeV^{-1}.

5 Conclusions

From the analysis of the events that have two leptons and one or more energetic photons in the final state, limits have been obtained on the masses and couplings of excited charged leptons decaying into a normal lepton and a photon. The non-observation of the pair production of these particles sets lower limits on their mass that reach 45.6 GeV/c^2. The results of the search for single production allow the exclusion of masses below 85 GeV/c^2 for e^*, 77 GeV/c^2 for μ^* and 63 GeV/c^2 for τ^*, as long as the scale that characterizes the l^*lZ and $l^*l\gamma$ couplings is smaller than 1 TeV.

Acknowledgements. We are greatly indebted to our technical collaborators and to the funding agencies for their support in building and operating the DELPHI detector, and to the members of the CERN-SL Division for the excellent performance of the LEP collider.

References

1. For a recent review on the subject see, for instance: F. Boudjema et al.: Z^0 Physics at LEP 1 (ed. G. Altarelli et al.), CERN 89-08 Vol. 2, p. 185–211
2. K. Hagiwara et al.: Z. Phys. C – Particles and Fields 29 (1985) 115
3. DELPHI Coll., P. Aarnio et al.: Nucl. Instrum. Methods A303 (1991) 233
4. DELPHI Coll., DELPHI Event Generation and Detector Simulation – User's Guide, DELPHI Note 89–67 (1989), unpublished
5. J. Cuevas et al.: Nucl. Instrum. Methods A274 (1989) 459
6. DELPHI Coll., P. Abreu et al.: Determination of Z^0 resonance parameters and couplings from its hadronic and leptonic decays, CERN-PPE/91–95 (1991), to be published in Nucl. Phys. B
7. S. Jadach, J. Was: Comp. Phys. Comm. 36 (1985) 191; S. Jadach et al.: Z^0 Physics at LEP 1 (ed. G. Altarelli et al.), CERN 89-08, vol. 3, p. 67
8. For $\mu\mu\gamma$ and $\tau\tau\gamma$ the KORALZ Monte Carlo was used; and for $ee\gamma$, the BABAMC generator, described in F.A. Berends, W. Hollik, R. Kleiss: Nucl. Phys. B304 (1988) 712
9. M.S. Chen, P. Zerwas: Phys. Rev. D 12 (1975) 187
10. DELPHI Coll., P. Abreu et al.: Phys. Lett. B247 (1990) 157
11. F.M. Renard: Phys. Lett. B116 (1982) 264; F. del Aguila, A. Méndez, R. Pascual: Phys. Lett. B140 (1984) 431; M. Suzuki: Phys. Lett. B143 (1984) 237
12. ALEPH Collab., D. Decamp et al.: Phys. Lett. B236 (1990) 501; OPAL Coll., M.Z. Akrawy et al.: Phys. Lett B244 (1990) 135; L3 Coll., B. Adeva et al.: Phys. Lett. B247 (1990) 177; Phys. Lett. B250 (1990) 205
13. DELPHI Coll., P. Abreu et al.: Phys. Lett. B 268 (1991) 296